



ELSEVIER

Catalysis Today 45 (1998) 85–92



# Transient kinetic study of the SCR-DeNO<sub>x</sub> reaction

Luca Lietti<sup>\*</sup>, Isabella Nova, Enrico Tronconi, Pio Forzatti

*Dipartimento di Chimica Industriale e Ingegneria Chimica, Politecnico di Milano, P.zza L. Da Vinci 32, 20133 Milano, Italy*

## Abstract

The unsteady-state kinetics of the selective catalytic reduction (SCR) of NO with NH<sub>3</sub> is studied over V<sub>2</sub>O<sub>5</sub>–WO<sub>3</sub>/TiO<sub>2</sub> model catalysts by means of the transient response method. NH<sub>3</sub> strongly adsorbs onto the catalyst surface whereas NO does not adsorb appreciably. A dynamic mathematical model based on a Temkin-type desorption process for NH<sub>3</sub> and a SCR reaction rate with a complex dependence on the ammonia surface coverage is well suited to represent the data. © 1998 Elsevier Science B.V. All rights reserved.

**Keywords:** Selective catalytic reduction (SCR); Vanadia-based catalysts; Transient kinetic study; Ammonia adsorption-desorption; SCR, dynamic model

## 1. Introduction

The NO<sub>x</sub> removal from the flue gases of stationary sources (DeNO<sub>x</sub>ing) is efficiently achieved by using the SCR (selective catalytic reduction) technique. In this process, ammonia is injected in the flue gases and NO<sub>x</sub> are eliminated via following reaction [1,2]:



Operation of industrial SCR reactors often involves transient conditions associated e.g. with load variations and start-up or shut down of the plant. Also, the SCR technology has been proposed for NO<sub>x</sub> abatement in systems characterized by fast load changes, such as diesel engines [3,4].

Accordingly, a study of the DeNO<sub>x</sub> reaction under non-stationary conditions has been undertaken in our labs, aiming at obtaining additional insight on the

dynamics of the SCR process and on the mechanistic features of the reaction under both steady- and unsteady-state conditions. For this purpose, the transient response method [5] has been applied: perturbations are imposed to the reacting system (e.g. step changes in the inlet reactant concentration) and the transient response is analyzed. The characteristics of the response reflect the sequence of the elementary steps of the reaction, therefore, these methods are able to provide, in principle, mechanistic evidence that cannot be collected under steady-state conditions, where all the steps of the reaction are progressing at the same rate. Finally, in order to obtain quantitative kinetic indications, the results of the transient experiments have been analyzed according to a simple dynamic model of the reacting system.

## 2. Experimental

Sub-monolayer V<sub>2</sub>O<sub>5</sub>/TiO<sub>2</sub> (V<sub>2</sub>O<sub>5</sub>=1.47% w/w, θ<sub>V</sub>=0.21, S<sub>a</sub>=46 m<sup>2</sup>/g) and V<sub>2</sub>O<sub>5</sub>–WO<sub>3</sub>/TiO<sub>2</sub>

<sup>\*</sup>Corresponding author. Tel.: +39-02-23993272; fax: +39-02-70638173; e-mail: luca.lietti@polimi.it

( $V_2O_5=1.47\%$  w/w and  $WO_3=9\%$  w/w,  $\theta_V=0.12$ ,  $\theta_W=0.67$  and  $S_a=80\text{ m}^2/\text{g}$ ) model catalysts were used in this study. The transient experiments were performed in a flow-microreactor system, consisting in a small quartz tube (6 mm i.d.) connected to a mass spectrometer. The reactor contained 160 mg of catalyst (60–100 mesh). A stream of He+1% v/v  $O_2$  (120 cc/min STP) was used, containing 700 ppm  $NH_3$  and 700 ppm NO. Abrupt switches in the reactant feed concentration were performed by means of a four-port valve positioned at the reactor inlet. Further details on the catalyst preparation and characterization and on the apparatus can be found elsewhere [6,7].

### 3. Results and discussion

#### 3.1. Transient kinetics of $NH_3$ and NO adsorption–desorption

The dynamic adsorption–desorption of the SCR reactants (i.e.  $NH_3$  and NO) in flowing He+1% v/v  $O_2$  has been investigated at first. A typical result obtained in the case of a rectangular step feed of ammonia performed at  $220^\circ\text{C}$  over the  $V_2O_5$ – $WO_3$ /TiO<sub>2</sub> model catalyst is presented in Fig. 1(A), along with the ideal ammonia inlet concentration (dashed lines). Upon the  $NH_3$  step addition (at  $t=0$  s), the ammonia reactor outlet concentration slowly

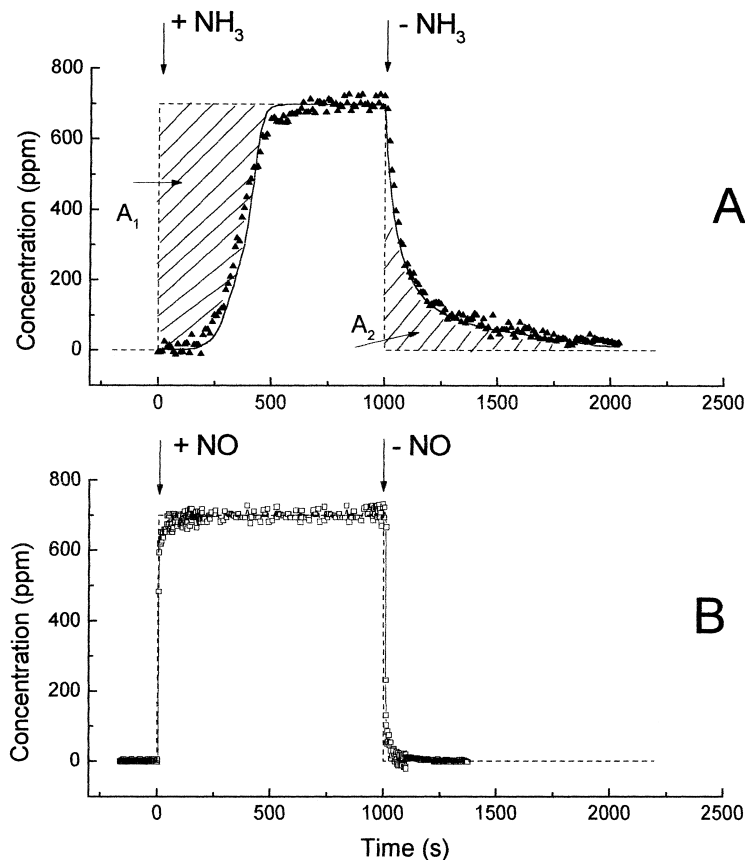


Fig. 1. Dynamic adsorption–desorption of  $NH_3$  (A) and NO (B) on a model  $V_2O_5$ – $WO_3$ /TiO<sub>2</sub> catalyst at  $220^\circ\text{C}$ . Dashed line: ideal step; solid lines: model fit.

increased with time, approaching the ammonia inlet concentration (700 ppm) only after  $\approx 500$  s. This clearly indicates that ammonia is involved in adsorption–desorption processes at the catalyst surface. Along similar lines, upon the ammonia shut-off ( $t=1000$  s) the reactor outlet  $\text{NH}_3$  concentration slowly decreases with time due to the desorption of previously adsorbed ammonia. Complete desorption of  $\text{NH}_3$  is not yet achieved after 2200 s, as shown by the lower value of area  $A_2$  if compared with  $A_1$ . This indicates that part of the pre-adsorbed ammonia is strongly adsorbed on the catalyst surface. The  $\text{NH}_3$  dynamic adsorption–desorption experiments were also performed at higher temperatures, in the range 220–400°C. On increasing the catalyst temperature, the variations in the ammonia outlet concentration during the adsorption step are faster and the amount of ammonia adsorbed on the catalyst surface is reduced, in line with the increased rates of the adsorption–desorption processes and with the exothermicity of the  $\text{NH}_3$  adsorption.

Rectangular inlet step feeds were also performed with NO, and a typical result is shown in Fig. 1(B). It appears that the reactor outlet NO concentration curves closely resemble that of the inlet NO concentration: this indicates that NO does not appreciably adsorb onto the catalyst surface, in line with literature data [8]. Similar results have also been obtained over the binary  $\text{V}_2\text{O}_5/\text{TiO}_2$  sample.

### 3.2. Transient kinetics of SCR of NO by $\text{NH}_3$

The dynamics of the SCR reaction has also been investigated. Accordingly, step feed experiments of  $\text{NH}_3$ , NO and  $\text{O}_2$  have been performed, while keeping constant the concentration of the other reactants. Fig. 2(A) shows a typical result obtained upon performing step changes of the  $\text{NH}_3$  reactor inlet concentration at 220°C in  $\text{He}+\text{NO}$  700 ppm+ $\text{O}_2$  1% v/v. The figure reports the evolution with time of  $\text{NH}_3$ ,  $\text{N}_2$  and NO concentrations.

Upon the  $\text{NH}_3$  step feed at  $t=0$  s, the NO reactor outlet concentration decreased due to the occurrence of the SCR reaction. The evolution with time of the ammonia, NO and  $\text{N}_2$  concentrations shows different transient behaviors: the  $\text{NH}_3$  concentration profile exhibits a dead time ( $\approx 250$  s) and then slowly increases with time on stream to the new steady-state

value, that is reached only after 800 s. On the other hand, the NO concentration trace does not show any dead time and decreases to its new steady-state value, reached after 300 s. The evolution with time of  $\text{N}_2$  and of  $\text{H}_2\text{O}$  (not reported in Fig. 2) is specular to that of NO. No formation of other species (e.g.  $\text{N}_2\text{O}$ ) was observed. It is worth of note that after 300 s, the reactor outlet NO concentration (and hence the NO conversion) is virtually constant, whereas the  $\text{NH}_3$  concentration is still increasing. This is a clear indication of the fact that the NO conversion does not depend on the ammonia surface coverage ( $\theta_{\text{NH}_3}$ ) for  $\theta_{\text{NH}_3}$  values above a characteristic ‘critical’ value.

A different transient behavior is observed upon the  $\text{NH}_3$  shut-off ( $t=1000$  s). Indeed whereas the  $\text{NH}_3$  concentration dropped to zero, the NO concentration signal was not apparently affected; only after several minutes it began to increase up to the inlet concentration value. Again this indicates that the rate of the SCR reaction does not depend on  $\theta_{\text{NH}_3}$  above a characteristic ‘critical’ value. The fact that NO is consumed even in the absence of gas-phase ammonia suggests that a ‘reservoir’ of adsorbed ammonia species available for the reaction is present on the catalyst surface.

Similar results were obtained by performing the  $\text{NH}_3$  step-feed experiments at higher temperatures (280 and 350°C). In particular on increasing the reaction temperature: (i) the steady-state NO conversion is increased, (ii) the  $\text{NH}_3$  and NO steady-state concentration levels are more rapidly reached; (iii) the ‘dead time’ in the variation of the NO concentration that is observed upon the ammonia shut-off (Fig. 2(A)) is reduced. Such temperature effects are in line with both the exothermicity of the  $\text{NH}_3$  adsorption and with the increased rate of the surface reaction, which result in lower ammonia surface coverage. Accordingly at low  $\theta_{\text{NH}_3}$  values the rate of NO consumption becomes dependent on the ammonia surface concentration, so that the evolution of NO closely follows that of  $\text{NH}_3$ .

The dynamic behavior of the SCR reaction upon step changes in the NO reactor inlet concentration has also been investigated. Fig. 2(B) show typical results obtained upon performing a rectangular step feed of NO at 493 K. Upon the NO step feed ( $t=0$  s) the  $\text{NH}_3$  reactor outlet concentration immediately decreases due to the occurrence of the SCR reaction, and a parallel evolution of  $\text{N}_2$  and of water (not reported

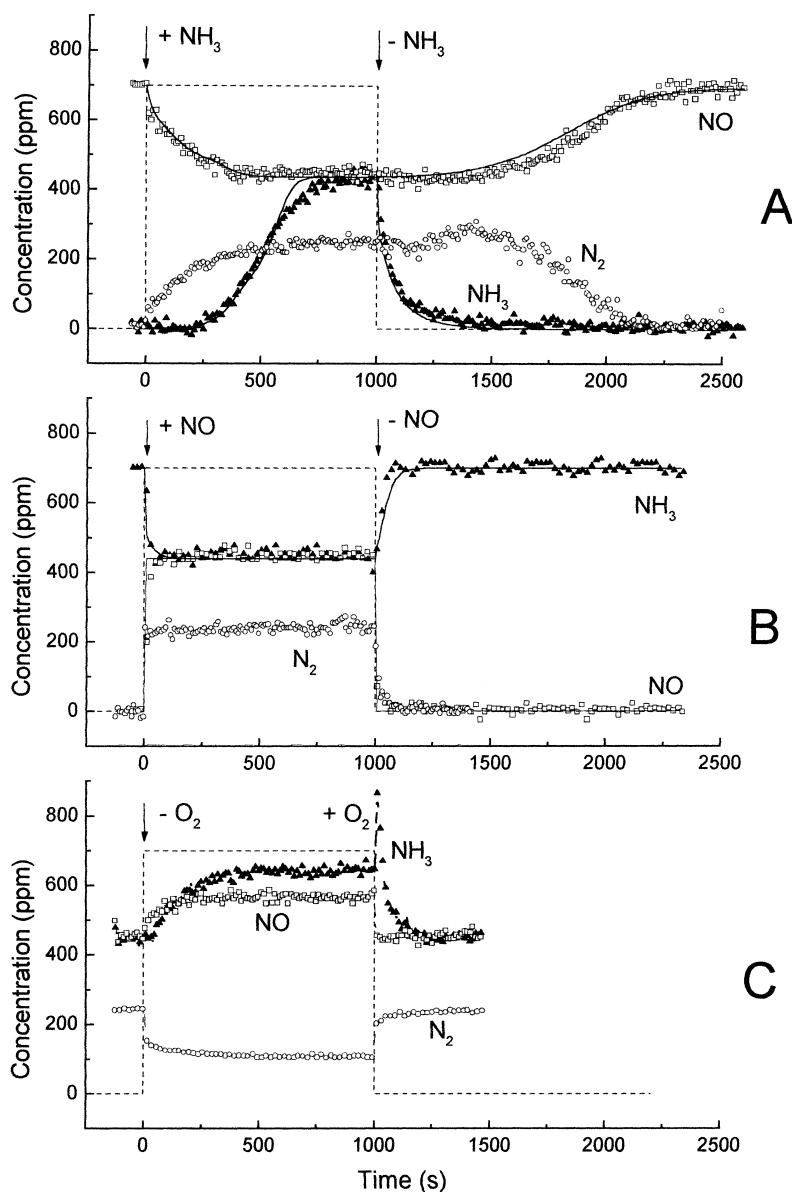


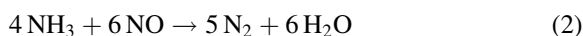
Fig. 2. Dynamic response upon step feed and shut-off of NH<sub>3</sub> (A), NO (B) and O<sub>2</sub> (C) on a model V<sub>2</sub>O<sub>5</sub>–WO<sub>3</sub>/TiO<sub>2</sub> catalyst at 220°C. Dashed line: ideal step; solid lines: model fit.

in the figure) is observed. Along similar lines, upon the NO shut-off, the NO, NH<sub>3</sub> and N<sub>2</sub> reactor outlet concentration reach their steady-state values immediately. This picture significantly differs from that observed during the corresponding NH<sub>3</sub> step feed experiments reported in Fig. 2(A). The observed transient responses are typical of a reaction involving a

strongly adsorbed species (NH<sub>3</sub>) and a gas-phase or weakly adsorbed species (NO). Indeed, upon the NH<sub>3</sub> admission and shut-off (Fig. 2(A)), the NO (and NH<sub>3</sub>) response is slow due to the fact that ammonia is involved in adsorption–desorption processes; on the other hand, the opposite is observed upon switches of NO (Fig. 2(B)). These data, along with the results of

the adsorption–desorption experiments shown in Fig. 1, are in line with the hypothesis of an Eley–Rideal mechanism for the SCR reaction involving strongly adsorbed  $\text{NH}_3$  and gas-phase or weakly adsorbed NO.

Finally, the role of oxygen in the SCR reaction has been investigated. Fig. 2(C) shows that upon the  $\text{O}_2$  shut-off at  $t=0$  s the  $\text{NH}_3$  concentration slowly increases to the new steady state value, whereas a more rapid transient behavior is observed for NO. It is also noted that in the absence of oxygen the  $\text{NH}_3$  and NO steady-state levels differs, in line with the following stoichiometry of the SCR reaction:



The  $\text{NH}_3$  transient response could be explained by considering that, due to the low rate of the SCR reaction in the absence of oxygen, higher  $\text{NH}_3$  surface coverage are expected and accordingly ammonia is adsorbed from the gas-phase until the new value is attained. On the other hand, the fact that the NO concentration does not reach the new steady-state value immediately, can be tentatively explained by considering that either adsorbed or catalyst lattice oxygen is available for the reaction so that the SCR reaction occurs via the faster reaction (1) instead of reaction (2). By assuming that only the vanadium catalyst lattice oxygen is involved in the reaction and that  $\text{V}^{5+}$  is reduced to  $\text{V}^{4+}$ , it is estimated that the reduction process involves roughly 3% of  $\text{V}^{5+}$ . This amount increases up to  $\sim 12\%$  when the  $\text{O}_2$  pulses are performed at  $280^\circ\text{C}$ .

Upon the  $\text{O}_2$  re-admission at  $t=1000$  s, NO rapidly reaches its new steady-state value whereas the reactor outlet  $\text{NH}_3$  concentration at first increases and then decreases to the steady-state level. This particular behavior can be tentatively explained by considering that upon the catalyst reoxidation the temperature of the catalyst is increased, thus leading to the observed  $\text{NH}_3$  desorption peak.

The data presented in Fig. 2 clearly show that the SCR reaction is faster in the presence of oxygen than in its absence, since a higher NO conversion is attained. This is in line with the well known promoting effect of the gas-phase oxygen on the SCR reaction. As pointed out in previous works [9–11] the SCR reaction occurs via a redox mechanism, which involves at first the catalyst lattice oxygen, followed

by catalyst reoxidation by gas-phase oxygen. Oxygen accelerates the SCR reaction by increasing the rate of the reoxidation process, which in the absence of oxygen is carried out by NO. Several data have been reported in the literature concerning the possible role of oxygen in the NO oxidation and adsorption on the catalyst surface, but this feature seems to be more likely for Cu- [12–14], Cr- [15] or Mn-based [16,17] catalysts. As matter of facts, our data show that NO is not appreciably adsorbed on the catalyst surface even in the presence of oxygen (see Fig. 1), thus apparently ruling out a mechanism which involves NO oxidation and adsorption on the catalyst surface.

### 3.3. Kinetic analysis of the transient experiments

The results of the dynamic  $\text{NH}_3$  adsorption–desorption and of the  $\text{NH}_3$  and NO step feed experiments performed at different temperatures have been analyzed according to a dynamic one-dimensional heterogeneous PFR model and fitted by non linear regression to provide estimates of the relevant kinetic parameters. The  $\text{O}_2$  transient experiments have not been analyzed and accordingly only qualitative information have been derived from these experiments. On the basis of diagnostic criteria, the influence of both intraparticle catalyst gradients and external mass transfer limitations were found negligible. Under these hypotheses, the unsteady mass balance of  $\text{NH}_3$  on the catalyst surface and of  $\text{NH}_3$  and NO in the gas-phase were written (Eqs. (1–3) of Table 1, respectively), where  $C_{\text{NH}_3}$  and  $C_{\text{NO}}$  represent the  $\text{NH}_3$  and NO gas-phase concentration, respectively;  $r_a$ ,  $r_d$  and  $r_{\text{NO}}$  the rate of adsorption, desorption and of NO consumption, respectively;  $v$  is the interstitial gas velocity,  $z$  the reactor axial coordinate and  $\Omega$  the catalyst  $\text{NH}_3$  adsorption capacity. On the basis of

Table 1  
Unsteady mass balances of  $\text{NH}_3$  on the catalyst surface (1) and of  $\text{NH}_3$  (2) and NO (3) in the gas phase

---


$$\frac{\partial \theta_{\text{NH}_3}}{\partial t} = r_a - r_d - r_{\text{NO}} \quad (1)$$

$$\frac{\partial C_{\text{NH}_3}}{\partial t} = -v \frac{\partial C_{\text{NH}_3}}{\partial z} + \Omega(r_d - r_a) \quad (2)$$

$$\frac{\partial C_{\text{NO}}}{\partial t} = -v \frac{\partial C_{\text{NO}}}{\partial z} - \Omega r_{\text{NO}} \quad (3)$$


---

preliminary fits of the experimental data, it was found that the  $\text{NH}_3$  adsorption occurs via a non-activated process, described by the rate expression  $r_a = k_a^o C_{\text{NH}_3} (1 - \theta_{\text{NH}_3})$ , with  $k_a^o = \text{constant}$ . An activated kinetic rate expression was instead used for  $\text{NH}_3$  desorption ( $r_d = k_d^o \exp(-E_d/RT) \theta_{\text{NH}_3}$ ). Different dependence of  $E_d$  on  $\theta_{\text{NH}_3}$  have been used, including  $E_d = \text{constant}$  (Langmuir) and more complicate expressions that take into account the catalyst surface heterogeneity. These included Temkin-type ( $E_d = E_d^o (1 - \alpha \theta_{\text{NH}_3})$ ), modified Temkin-type ( $E_d = E_d^o (1 - \alpha \theta_{\text{NH}_3}^o)$ ) and Freundlich ( $E_d = E_d^o \exp(-\alpha \theta_{\text{NH}_3})$ ) coverage dependence of  $E_d$ , along with more complicate empirical expressions. Also, different rate expressions have been tested for the SCR reaction ( $r_{\text{NO}}$ ). These always include a first order dependency on  $C_{\text{NO}}$ , and various order dependencies with respect to  $\theta_{\text{NH}_3}$ , including first-order ( $r_{\text{NO}} = k_{\text{NO}} C_{\text{NO}} \theta_{\text{NH}_3}$ ) and ‘modified’  $\theta$  kinetics ( $r_{\text{NO}} = k_{\text{NO}} C_{\text{NO}} \theta_{\text{NH}_3}^* [1 - \exp(-\theta_{\text{NH}_3}/\theta_{\text{NH}_3}^*)]$ ). In this case the rate of reaction is considered independent on  $\theta_{\text{NH}_3}$  above a critical  $\text{NH}_3$  surface concentration value ( $\theta_{\text{NH}_3}^*$ ), in line with the results of the  $\text{NH}_3$  step addition experiments reported in Fig. 2(A). Nice fits of the experimental data for both the binary and the ternary catalysts could be achieved by using a Temkin-type  $\text{NH}_3$  desorption kinetics (the Langmuir approach fails in quantitatively describing the experimental data) and the ‘modified’  $\theta$  kinetics for  $r_{\text{NO}}$ . A typical data fit obtained in the case of the ternary sample is reported as solid line in Figs. 1 and 2, whereas the estimates of the kinetic parameters used in the data fit

are reported in Table 2, along with those corresponding to the binary sample. The optimal parameter estimates yield an activation energy for  $\text{NH}_3$  desorption at zero coverage ( $E_d^o$ ) close to 25 kcal/mol for both catalysts. The slightly higher value of the catalyst capacity ( $\Omega = 270$  vs.  $209 \text{ mol}_{\text{NH}_3}/\text{m}^3$ ) of the ternary catalyst may be due to its higher specific surface area with respect to the  $\text{V}_2\text{O}_5/\text{TiO}_2$  binary sample (80 vs.  $46 \text{ m}^2/\text{g}$ ). An activation energy for the SCR reaction close to 15 kcal/mol has been estimated for both catalysts, in agreement with literature values [18].

### 3.4. Relevance to the study of kinetic and mechanistic aspects of the SCR reaction

The results of the dynamic study previously reported are in many respect relevant to the study of both kinetic and mechanistic aspects of the SCR reaction. It is worth emphasizing that these aspects could not be collected under steady-state conditions, and points out that dynamic conditions are best suited for mechanistic study of complex reactions. In particular, the  $\text{NH}_3$  dynamic adsorption–desorption study demonstrated that ammonia is strongly adsorbed on the catalyst surface and that surface heterogeneity must be considered when describing the  $\text{NH}_3$  interaction with the catalyst surface. This is in line with various characterization data showing the presence of different adsorption sites for ammonia, including Lewis and Brønsted acid sites [19,20]. Similar results have been obtained over both the binary and the ternary catalyst, thus eventually indicating that the acid characteristics of the two samples, with respect to the  $\text{NH}_3$  adsorption–desorption, are similar.

The study of the dynamics of the SCR reaction showed that the  $\text{DeNO}_x$  reaction has a complex kinetic dependence on the ammonia surface coverage. Indeed the rate of the SCR reaction is a function of the ammonia surface concentration for  $\text{NH}_3$  coverage below a characteristic ‘critical’ value, whereas a much weaker dependence exists at high coverage. As already suggested above, this indicates that a ‘reservoir’ of adsorbed ammonia species is present on the catalyst surface. The ammonia ‘reservoir’ is likely associated with the W and Ti surface species that are exposed at the catalyst surface in the case of the sub-

Table 2

Estimates of the kinetic parameters for the SCR reaction over  $\text{V}_2\text{O}_5/\text{TiO}_2$  and  $\text{V}_2\text{O}_5\text{--WO}_3/\text{TiO}_2$  catalysts leading to the fits reported in Figs. 1 and 2 (solid lines). Rate equations:  $r_a = k_a^o C_{\text{NH}_3} (1 - \theta_{\text{NH}_3})$ ;  $r_d = k_d^o \exp(-E_d/RT) \theta_{\text{NH}_3}$  with  $E_d = E_d^o (1 - \alpha \theta_{\text{NH}_3})$ ;  $r_{\text{NO}} = k_{\text{NO}} C_{\text{NO}} \theta_{\text{NH}_3}^* [1 - \exp(-\theta_{\text{NH}_3}/\theta_{\text{NH}_3}^*)]$

Parameters	$\text{V}_2\text{O}_5\text{--WO}_3/\text{TiO}_2$	$\text{V}_2\text{O}_5/\text{TiO}_2$
$k_a^o$ ( $\text{m}^3/\text{mol s}$ )	0.614	0.820
$k_d^o$ (1/s)	$1.99 \times 10^5$	$3.67 \times 10^6$
$E_d^o$ (kcal/mol)	23.4	25.8
$\alpha$	0.448	0.310
$\Omega$ ( $\text{mol}/\text{m}^3$ )	270	209
$k_{\text{NO}}^o$ ( $\text{m}^3/\text{mol s}$ )	$8.39 \times 10^5$	$1.08 \times 10^6$
$E_{\text{NO}}$ (kcal/mol)	14.2	16.0
$\theta_{\text{NH}_3}^*$	0.108	0.076

monolayer samples investigated in the present study. These species effectively adsorb  $\text{NH}_3$ , but their reactivity in the SCR reaction is limited [8,21] with respect to the V sites. Accordingly, these Ti- and W-bonded adsorbed ammonia species do not act as ‘spectators’ in the SCR reaction but can be involved in the NO consumption via desorption and subsequent fast re-adsorption over available reactive V-sites, in line with the results of the kinetic analysis.

The dynamic behavior of the SCR reaction could be nicely fitted by assuming a first order dependence on NO and a more complex dependence on the ammonia surface concentration (zero-order at high  $\text{NH}_3$  coverage and first-order below a ‘critical’ coverage  $\theta_{\text{NH}_3}^*$ ). This suggests that the catalyst active sites represent only a fraction of the total adsorption sites for ammonia. As a matter of fact, in line with the hypothesis of V being the active element in the SCR reaction, it has been found that the ‘critical’  $\text{NH}_3$  coverage  $\theta_{\text{NH}_3}^*$  is of the same order of magnitude of the catalyst V coverage. An important implication of the mechanistic considerations reported above is that in developing a kinetic model a distinction should be made between ammonia ‘adsorption’ and ‘reaction’ sites. Finally, the analysis of the parameter estimates obtained over both the binary and the ternary samples leads to additional implications concerning the steady-state kinetics of the SCR reaction. Indeed, being at steady-state  $r_a = r_d + r_{\text{NO}}$ , it follows that  $r_a \approx r_d$  (i.e.  $\text{NH}_3$  adsorption–desorption equilibrium) only if  $r_{\text{NO}}$  is negligible with respect to  $r_d$  ( $r_{\text{NO}} \ll r_d$ ). From the values of the kinetic parameters reported in Table 1 it is possible to estimate the  $r_d/r_{\text{NO}}$  ratios at different reactor axial position, different reaction temperatures and for different catalysts. It has been found that the values of the  $r_d/r_{\text{NO}}$  ratio do not change significantly between the inlet and the outlet of the reactor, and decrease upon increasing the temperature. The  $r_d/r_{\text{NO}}$  ratio is greater than 1 at 553 K and in the case of the less active vanadia/titania catalyst ( $r_d/r_{\text{NO}} \sim 10$ ) but it is close to 1 at the same temperature over the most active vanadia–tungsta/titania catalyst. This demonstrates that the assumption of equilibrated ammonia adsorption, often used in the derivation of steady-state kinetic expressions for the SCR [22], is in fact not always appropriate, and specifically at high temperatures and over very active catalysts, where not a single rate controlling step can be identified.

#### 4. Conclusions

The major results of our study can be summarized as follows:

1. Surface heterogeneity must be considered to describe the kinetics of  $\text{NH}_3$  adsorption–desorption on  $\text{TiO}_2$ -supported  $\text{V}_2\text{O}_5$ -based catalysts: a model assuming a non-activated  $\text{NH}_3$  adsorption process and a Temkin-type coverage dependence of  $E_d$  nicely represents the dynamic data.
2. In contrast to  $\text{NH}_3$ , NO does not adsorb appreciably on the catalyst surface, in line with an Eley-Rideal mechanism for the SCR reaction.
3. The rate of the  $\text{DeNO}_x$  reaction is virtually independent on the  $\text{NH}_3$  surface concentration for  $\theta_{\text{NH}_3}$  above a characteristic ‘critical’ value that is of the same order of magnitude of the V surface coverage. This is explained by assuming that a ‘reservoir’ of adsorbed  $\text{NH}_3$  species (likely on W and Ti sites) is present on the catalyst surface and is available for the reaction via desorption and subsequent fast re-adsorption over reactive V-sites, in line with the results of the kinetic analysis.
4. A comparison among the estimates of the adsorption, desorption and reaction rates calculated at different reactor axial position, temperatures and catalysts indicates that the assumption of equilibrated ammonia adsorption under steady-state  $\text{DeNO}_x$  conditions is likely incorrect, specifically at high temperatures and over active catalysts.

#### References

- [1] H. Bosch, F. Janssen, Catal. Today 2 (1988) 369.
- [2] P. Forzatti, L. Lietti, Heter. Chem. Rev. 3(1) (1996) 33.
- [3] S.L. Andersson, P.L.T. Gabrielsson, C.U.I. Odenbrand, AIChE. J. 40(11) (1994) 1911.
- [4] A. Noskov, L. Bobrova, G. Bunimovich, O. Goldman, A. Zagoruiko, Y. Matros, Catal. Today 27 (1996) 315.
- [5] H. Kobayashi, M. Kobayashi, Catal. Rev. Sci. Eng. 10 (1974) 139.
- [6] L. Alemany, L. Lietti, N. Ferlazzo, P. Forzatti, G. Busca, E. Giamello, F. Bregani, J. Catal. 155 (1995) 117.
- [7] L. Lietti, I. Nova, S. Camurri, E. Tronconi, P. Forzatti, AIChE. J. 43(10) (1997) 2559.
- [8] T.Z. Smak, J.A. Dumesic, B.S. Clausen, E. Törnqvist, N.Y. Topsøe, J. Catal. 135 (1992) 246.
- [9] L. Lietti, P. Forzatti, F. Berti, Catal. Lett. 41 (1996) 35.

- [10] L. Lietti, P. Forzatti, F. Bregani, *Ind. Eng. Chem. Res.* 35(11) (1996) 3884.
- [11] L. Lietti, P. Forzatti, *J. Catal.* 147 (1994) 241.
- [12] G. Ramis, Yi Li, G. Busca, M. Turco, E. Kotur, R.J. Willey, *J. Catal.* 157 (1995) 523.
- [13] G. Centi, S. Perathoner, P. Biglino, E. Giamello, *J. Catal.* 152 (1995) 75.
- [14] G. Centi, S. Perathoner, P. Biglino, E. Giamello, *J. Catal.* 152 (1995) 93.
- [15] H. Schneider, U. Scharf, A. Wokaun, A. Baiker, *J. Catal.* 147 (1994) 545.
- [16] F. Kapteijn, L. Singoredjo, M. van Driel, A. Andreini, J.A. Moulijn, G. Ramis, G. Busca, *J. Catal.* 150 (1994) 105.
- [17] F. Kapteijn, L. Singoredjo, A. Andreini, J.A. Moulijn, *Appl. Catal. B: Environ.* 3 (1994) 173.
- [18] W.C. Wong, K. Nobe, *Ind. Eng. Chem. Prod. Res. Dev.* 23 (1984) 564.
- [19] G. Ramis, G. Busca, F. Bregani, P. Forzatti, *Appl. Catal.* 64 (1990) 259.
- [20] N.-Y. Topsøe, *J. Catal.* 128 (1991) 499.
- [21] L. Lietti, *Appl. Catal. B: Environ.* 10 (1996) 281.
- [22] J.A. Dumesic, N.-Y. Topsøe, T. Slabak, P. Morsing, B.S. Clausen, E. Tornqvist, H. Topsøe, in: L. Guzzi, et al. (Eds.), *New Frontiers in Catalysis*, Elsevier, Amsterdam, 1992, 1325 pp.